Proceedings of the 1998 IEEE
International Conference on Robotics & Automation
Leuven, Belgium • May 1998

Autonomous Land Vehicle Navigation Using Millimeter Wave Radar

S.Clark
Australian Centre for Field Robotics
Sydney University, Australia
clark@mech.eng.usyd.edu.au

H.Durrant-Whyte
Australian Centre for Field Robotics
Sydney University, Australia
hugh@mech.eng.usyd.edu.au

This work was conducted as part of the "Field Automation" research program of the Cooperative Research Centre for Mining Technology and Equipment (CMTE)

Abstract

This paper discusses the use of a 77GHz millimeter wave radar as a guidance sensor for autonomous land vehicle navigation. A test vehicle has been fitted out with a radar and encoders that give steer angle and velocity. An extended Kalman filter optimally fuses the radar range and bearing measurements with vehicle control signals to give estimated position and variance as the vehicle moves around a test site. The effectiveness of this data fusion is compared with encoders alone and with a satellite positioning system. Consecutive scans have been combined to give a radar image of the surrounding environment. Data in this format will be invaluable for future work on collision detection and map building navigation.

1 Introduction

Millimetre wave (MMW) radar satisfies many of the criteria required of a sensor in high performance outdoor autonomous vehicle navigation. The short wavelength, compared to microwave radar provides high resolution measurements. MMW radar is also able to operate in adverse weather and environmental conditions compared to optical sensors such as lasers. With modern digital processing techniques, it is possible to locate navigation targets at greater distances than other sensors with a high degree of accuracy. The high bandwidth of the radar intermediate frequency (IF) allows measurements of sufficient range and resolution to maintain high quality, high rate updates for a vehicle navigation algorithm. Extra information can be extracted from the polarisation of the radar signal to enable navigation targets to be distinguished from clutter. This paper describes a high-performance MMW radar navigation system, exploiting many of the potential advantages of this type of radar as a primary navigation sensor. The system described differs substantially from the collision detection radars currently being developed for automotive applications [4]in a number of ways. First, the unit has much higher range and bearing accuracy than those commonly deployed. Second, the system is capable both of high-precision position determination and of generating full amplitude radar images for use in terrain mapping.

The design and essential measurement principles of the front-end radar unit are described in Section 2. Section 3 describes the fusion of radar range and bearing measurements with encoder readings in an extended Kalman filter to estimate the vehicles state. Section 4 presents the results of measurements made from the position determination system. In conclusion, Section 5.

2 The Radar System

The radar employed in this paper has a 77 GHz baseband frequency, the designated automotive frequency in Europe and the United States, chosen for its low atmospheric absorption. Figure 1 shows how the carrier wave is frequency modulated (FMCW) over 600 MHz in 1mS. The reflected signal is also shown on an expanded time scale. The time between transmission and reception of the radar signal gives a measure of the distance to the reflecting surface, however given the limited maximum range it is not practical to measure such small time intervals. Instead, transmitted and received MMW signals are mixed and the frequency difference extracted, this intermediate frequency is a measure of the target distance. Equation 1 where Δf is the intermediate frequency, T_s and f_s the sweep time and frequency and c the speed of electromagnetic radiation.

$$Range = \frac{cT_s}{2f_s}\Delta f \qquad (1)$$

The maximum range measurable depends on the maximum IF bandwidth that can be processed and the radar sweep time and swept frequency. The MMW radar unit described in this paper employs a 36db lens antenna yielding a beam divergence of approximately 1.2^o. For this reason, a maximum radar range of 250 meters was selected since the beam width at this range will be in the order of meters making it difficult to accurately locate targets. With a 1mS sweep a 250 meter range corresponds to 1Mhz bandwidth, providing an unprocessed range accuracy of 0.25m. The front-end unit also exploits a dual polarisation receiver to discriminate between navigation targets and ground clutter. [2] includes a more involved discussion of the radar and signal processing system.

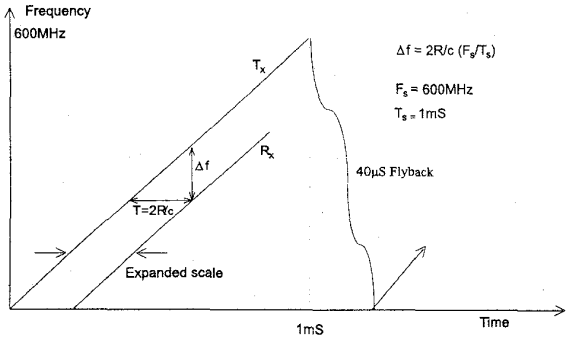

Figure 1: Radar chirp showing transmitted and received frequencies, the difference between these provides a range measurement

2.1 The test vehicle

A Holden Utility vehicle has been fitted out for the purpose of testing a selection of guidance sensors. Figure 2 shows the location of the radar on the center line of the vehicle. Encoders have been fitted to the drive shaft which give a measure of the vehicles speed, an LVDT on the steering rack provides a heading measurement. Differential GPS equipment and an inertial navigation unit are also fitted to the vehicle. The intention is to have the radar/encoder navigation filter running in parallel with the GPS/INS filter. The redundant vehicle location estimates will be fused to provide a robust navigation system with centimeter accuracy in all operating conditions. At present the system is capable of logging measurements from all the sensors for offline processing. The radar system incorporates a high end digital signal processor, however logging hardware is transputer based.

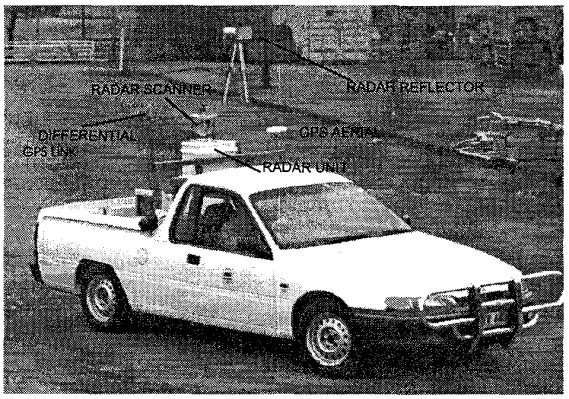

Figure 2: Vehicle with radar and GPS mounted

3 Vehicle Navigation

Vehicle localisation is performed with the well known extended Kalman filter algorithm (EKF) [6].In this discussion familiarity with the EKF and the standard notation is assumed. With reference to figure 3.

3.1 Process Model

The Vehicle state, $\mathbf{x}(k-1)$, consisting of x, y local and orientation of the vehicle is propagated to time (k) through a process model. This model takes the control inputs to the vehicle and estimates vehicle state at (k) together with the uncertainty in vehicle location, represented in the $\mathbf{P}(k)$ covariance matrix.

$$\hat{\mathbf{x}}(k|k-1) = \mathbf{f}(\mathbf{x}(k-1), \mathbf{u}(k)) + \mathbf{v}(k) \qquad (2)$$

The control signals applied to the vehicle are measured $\mathbf{u}(k) = [V(k), \gamma(k)]$. $V(k)$ is the velocity and $\gamma(k)$ is the steer angle, B is the length of the vehicle wheelbase. ΔT is the time interval between states at $(k-1)$ and (k). $\mathbf{v}(k)$ is additive process noise.

$$\begin{bmatrix} \hat{x}(k|k-1) \\ \hat{y}(k|k-1) \\ \hat{\Phi}(k|k-1) \end{bmatrix} = \begin{bmatrix} \hat{x}(k-1|k-1) \\ \hat{y}(k-1|k-1) \\ \hat{\Phi}(k-1|k-1) \end{bmatrix}$$

$$+\begin{bmatrix} V(k)\Delta T\cos(\hat{\Phi}(k-1|k-1)+\gamma(k)) \\ V(k)\Delta T\sin(\hat{\Phi}(k-1|k-1)+\gamma(k)) \\ \frac{V(k)\Delta T}{B}\sin(\gamma(k)) \end{bmatrix} \quad (3)$$

$\hat{x}(k|k-1)$ denotes the estimate of x at (k) given all information upto and including time step $(k-1)$. Errors in the estimate of $\mathbf{x}$ are introduced as noise on the control inputs to the model.

The extended Kalman filter linearises noise around the estimated position by taking the Jacobians of the process model. Noise existing at time $(k-1)$ is propogated through the linearised model, additional noise is added from the control inputs of the latest prediction in the $\mathbf{Q}(k)$ matrix. This is calculated by taking the Jacobians of the process model about the control vector, $\mathbf{u}(k)$.

Thus covariances are propagated through the model in the extended Kalman filter form for non-linear systems.

$$\mathbf{P}(k|k-1) = \nabla f_x(k)\mathbf{P}(k-1|k-1)\nabla f_x(k)^{\mathbf{T}} + \mathbf{Q}(k) \quad (4)$$

$$\nabla f_x(k) = \begin{bmatrix} 1 & 0 & -V(k)\Delta T\sin(\hat{\Phi}(k-1)+\gamma(k)) \\ 0 & 1 & V(k)\Delta T\cos(\hat{\Phi}(k-1)+\gamma(k)) \\ 0 & 0 & 1 \end{bmatrix} \quad (5)$$

As mentioned $\mathbf{Q}(k)$ is given by

$$\mathbf{Q} = \nabla f_u \Sigma_c \nabla f_u{}^{\mathbf{T}} \quad (6)$$

where $\Sigma_c = \begin{bmatrix} {\sigma_v}^2 & 0 \\ 0 & {\sigma_\gamma}^2 \end{bmatrix}$ includes the variances of the velocity and steer angle measurements.

The linearised process model around the control vector evaluated at $\hat{\mathbf{x}}(k)$ is $\nabla f_u(k)$

$$= \begin{bmatrix} \Delta T\cos(\Phi+\gamma) & -V(k)\Delta T\sin(\Phi+\gamma) \\ -\Delta T\sin(\Phi+\gamma) & V(k)\Delta T\cos(\Phi+\gamma) \\ \frac{\Delta T}{B}\sin(\gamma(k)) & \frac{V(k)\Delta T}{B}\cos(\gamma(k)) \end{bmatrix} \quad (7)$$

where $\cos(\Phi+\gamma)$ is $\cos(\hat{\Phi}(k-1)+\gamma(k))$
and $\sin(\Phi+\gamma)$ is $\sin(\hat{\Phi}(k-1)+\gamma(k))$

3.2 Observation Model

Once the vehicle pose is predicted a radar observation is used to estimate the vehicle state. The prediction and estimation are fused optimally during the filter update. Without observations the uncertainty in state would grow unbounded. The position of the preplaced radar beacons is surveyed with a theodolite and it is assumed that errors in their location are negligible. In this case only nine beacons were used, the maximum range of the radar was adequate for these to provide sufficient coverage. For each of the beacons in the map the range $r(k)$ and azimuth $\Theta(k)$ are determined from the predicted vehicle location, equations 11

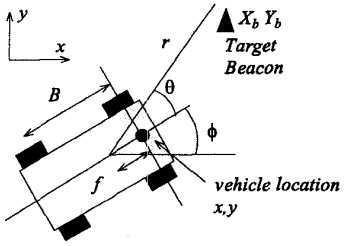

Figure 3: Beacon observation from the vehicle

The observations are modeled in the usual way,

$$\mathbf{z}(k) = \mathbf{h}(\mathbf{x}(k)) + \omega(k) \quad (8)$$

where $\mathbf{z}(k)$ is the observation, $\mathbf{h}$ is the observation model and $\omega(k)$ is additive observation noise. An innovation, $\nu(k)$ is calculated, the difference between actual observation, $\mathbf{z}(k)$ and expected observation given $\hat{\mathbf{x}}(k)$ and a known target location. Associated with the innovation is a covariance matrix $\mathbf{S}(k)$.

$$\nu(k) = \mathbf{z}(k) - \mathbf{h}(\hat{\mathbf{x}}(k|k-1)) \quad (9)$$

$\mathbf{S}(k)$, is calculated using the linearised observation model about the estimated position.

$$\mathbf{S}(k) = \nabla h_x(k)\mathbf{P}(k|k-1)\nabla h_x(k)^{\mathbf{T}} + \mathbf{R}(k) \quad (10)$$

where $\mathbf{R}(k) = E[\omega\omega^{\mathbf{T}}]$ is the noise variance matrix of the observations. $\mathbf{X}_b$ and $\mathbf{Y}_b$ give the beacon location in global co-ordinates and f is the distance from the vehicle location reference to the radar sensor. $\mathbf{X}mTx = \hat{\mathbf{x}}(k|k-1) - \mathbf{X}_b$, $\mathbf{T}ymY = \mathbf{Y}_b - \hat{\mathbf{y}}(k|k-1)$, $fc\Phi = f\cos\hat{\Phi}(k|k-1)$ and $fs\Phi = f\sin\hat{\Phi}(k|k-1)$

$$\begin{aligned} r(k) &= ((-\mathbf{X}mTx + fc\Phi)^2 + (\mathbf{T}ymY + fs\Phi)^2)^{0.5} \\ \Theta(k) &= \arctan(\frac{\mathbf{T}ymY + fs\Phi}{-\mathbf{X}mTx + fc\Phi}) - \hat{\Phi}(k|k-1) \end{aligned} \quad (11)$$

The elements of ∇h_x are shown in equations 12

$$\frac{\partial r}{\partial x} = \frac{\mathbf{X}mTx - fc\Phi}{r} \qquad \frac{\partial r}{\partial y} = \frac{-\mathbf{T}ymY - fs\Phi}{r}$$
$$\frac{\partial r}{\partial \Phi} = \frac{(\mathbf{X}mTx + fc\Phi)fs\Phi - (\mathbf{T}ymY + fs\Phi)fc\Phi}{r}$$
$$\frac{\partial \Theta}{\partial x} = \frac{\mathbf{T}ymY + fs\Phi}{r^2} \qquad \frac{\partial \Theta}{\partial y} = \frac{\mathbf{X}mTx - fc\Phi}{r^2}$$
$$\frac{\partial \Theta}{\partial \Phi} = \frac{(\mathbf{X}mTxfc\Phi) - (\mathbf{T}ymYfs\Phi) - \mathbf{X}mTx^2 - \mathbf{T}ymY^2}{r^2} \tag{12}$$

for completeness the standard extended Kalman filter gain and update equations are given by

$$\hat{\mathbf{x}}(k|k) = \hat{\mathbf{x}}(k|k-1) + \mathbf{W}(k)\nu(k)$$
$$\mathbf{P}(k|k) = \mathbf{P}(k|k-1) - \mathbf{W}(k)\mathbf{S}(k)\mathbf{W}(k)^{\mathbf{T}}$$
$$\mathbf{W}(k) = \mathbf{P}(k|k-1)\nabla h_x^T(k)\mathbf{S}^{-1}(k) \tag{13}$$

Measurements of the control inputs are sampled twenty times a second. If no radar observation is available between measurements the vehicle location is predicted forward with these alone. Observations will generally occur less frequently than the filter update rate and will rarely be synchronised. If a target is observed, the prediction must be carried forward to the time of the observation. Since all incoming data to the filter is timestamped in the logging computer, this is easily achieved. Once the observation and prediction are fused this new estimate is predicted forward to to be in sync with $20Hz$ prediction cycle.

3.3 Target Validation and Update

All measurements from the radar must be strictly validated to ensure they correspond to a known target location. Localising the vehicle on a falsely assigned target is catastrophic and the filter will not recover without reference to external sensor data.

The innovation sequence is validated probabilistically by gating the normalised innovation sequence [1]. If the filter is consistent the innovation will follow a χ^2 distribution.

$$\nu^T(k)\mathbf{S}^{-1}(k)\nu(k) \leq \gamma \tag{14}$$

For every observation the innovation and innovation covariance is calculated for each target. This shifting of the targets into a vehicle based co-ordinate system is adequate for the small number of targets used in this system. With greater target numbers however it would be more efficient to shift the innovation into global co-ordinates. The target locations are necessarily stored in global co-ordinates and the update must be accomplished in vehicle co-ordinates. An update in global co-ordinates is excessively sensitive to approximations in orientation uncertainty [5].

Only in the case where a single target satisfies equation 14 is the association of an observation with a particular target made. In this way only high quality observations are accepted and the integrity of the filter is maintained.

4 Experimental Data

Omnidirectional radar reflectors, comprising a modified diplane arrangement were surveyed into the test site. Data from all the vehicle sensors was recorded for several laps around the site. The data included GPS, radar, velocity and steer angle encoders as well as an inertial navigation unit. When tuning the prediction model to asses any bias in the control encoders the GPS data was a useful reference. Figure 4 shows the track taken by the vehicle as it moves through a grid of beacons, indicated by a $*$. The solid line indicates the estimated position of the vehicle calculated from the fused encoder and radar information. The dots are the position estimated position of the vehicle from the GPS data. Since the GPS antenna is located away from the vehicle model centre, midway between the front wheels, a transformation has been applied to shift the GPS data, allowing an accurate comparison. The vehicle starts moving at (0,0) counter clockwise then returns to the start position. The vehicle was moving for 53 seconds and 186 targets were successfully matched in that time and used to reset the vehicle position.

The covariances of the state vector indicate the uncertainty in state estimate over time, with each radar observation the covariance decreases. If no observations are made the covariance will increase until eventuality the lack of confidence in the current position is so great that it is impossible to correctly assign future observation to physical target locations. Figure 5 shows the covarinace in each of the elements of $\hat{\mathbf{x}}$ growing unbounded. It appears that covariance can decrease even without observations. The overall covariance does increase but individual elements may decrease due to the change in orientation of the covariance ellipse as the vehicle turns. Note that the orientation covariance increases monotonically.

Figures 6 and 7 show the state covariance and innovation sequence for a vehicle travelling a similar circuit whilst simultaneously matching beacons. This

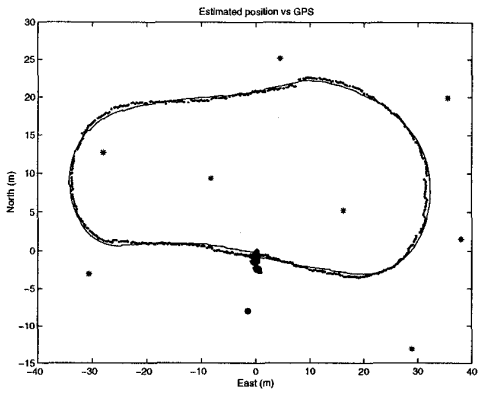

Figure 4: Beacon matching whilst moving in test site.

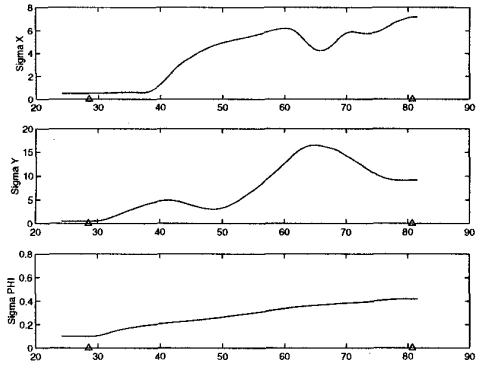

Figure 5: Unbounded growth in state covariance without observations.

model incorporated a 4 state filter using a wheel radius state to help account for any wheel slip/slide [5]. The initial uncertainty in vehicle state remains high from 0 to 24 seconds, then observation are made of the target beacons and the covariance decreases. The observation are evident in the innovation sequence at this time together with innovation covariance. Covariance of the wheel radius continues to increase, despite the observations until 28 seconds when the vehicle starts to move, figure 8. Wheel radius is unobservable whilst the vehicle is stationary. State Estimates are continually made as the vehicle travels around the site and the state covariances stay reasonably constant. The innovation sequence appears white with no obvious correlation or bias, this together with a comparison with the GPS 'true' state provide a good quality control of the data.

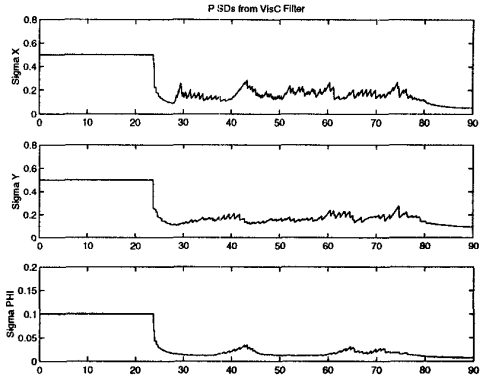

Figure 6: State covariances with a four state filter.

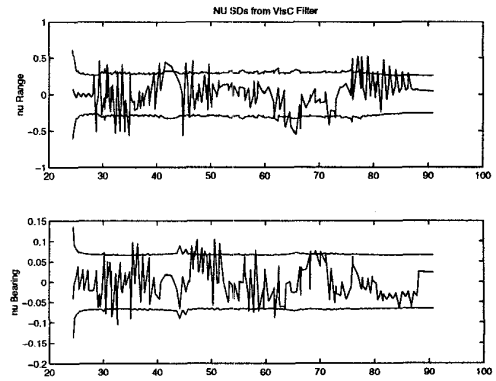

Figure 7: Innovation sequence with a four state filter.

4.1 Radar imaging

A succession of radar scans have been collected for post processing. Data in this format is very useful for comparing signal levels from the targets versus that from the clutter. Figure 9 shows such a scan from the test site, Beacons are identifiable as bright spots which indicate high signal strength at a particular range. In the lower left hand corner a container is stacked and provides high signal returns from the square edges. The test site is surrounded by an inclined rectangu-

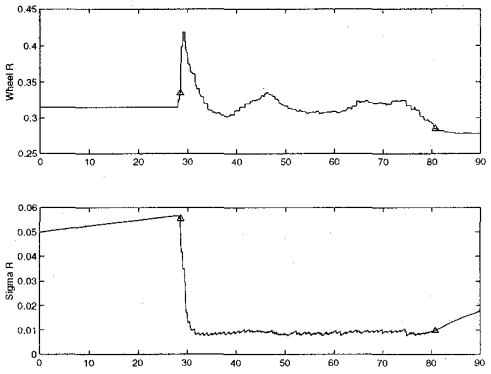

Figure 8: Wheel radius and wheel radius covariance.

lar earth bank which is clearly visible, as are several lightposts.

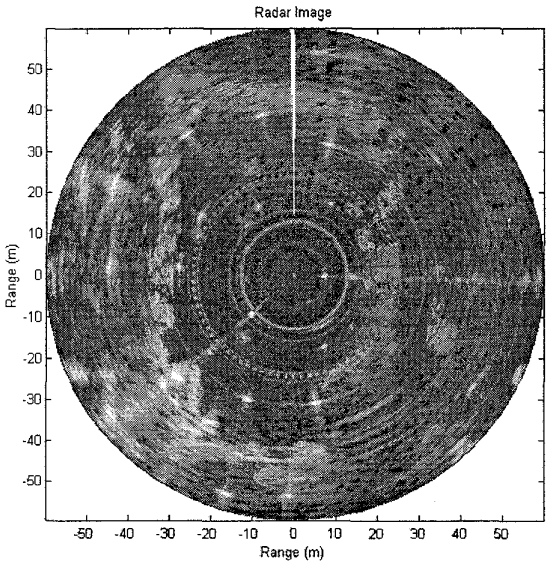

Figure 9: 360° Radar image tagen to 50 meters, sampled every 1.44°

5 Conclusions

The current navigation system matches preplaced beacons to localise. An improved method would eliminate the need for infrastructure by recognising features and building a map whilst simultaneously navigating. The validity of such an approach has been demonstrated to be feasible [3]. Features are clearly identifiable from the scanned image. Typical operating environments would include many similar structures that could be used as navigation waypoints.

In a future application the radar may be useful for imaging environments that are not easily observable with current sensors. Optical sensors usually fail to perform in dusty conditions or in rain and while radar images will have lower resolution gross features will still be detectable.

It has been possible to demonstrate the effectiveness of a MMW radar as a guidance sensor. Reflector beacons have been successfully identified from clutter at a sufficient rate to maintain an estimate of vehicle location. The data collected has been optimally fused with encoder information in an extended Kalman filter. The image data gives a useful insight into the visibility of objects to this sensor and provides a basis for future work.

References

[1] Y. Bar-Shalom and T.E. Fortman. *Tracking and Data Association.* Academic Press, 1988.

[2] S. Clark and H.F. Durrant-Whyte. The design of a high performance mmw radar system for autonomous land vehicle navigation. In *Proceedings of the International Conference on Field and Service Robotics*, December 1997.

[3] M. Csorba and H.F. Durrant-Whyte. A new approach to map building using relative position estimates. In *Proceedings of SPIE - The International Society for Optical Engineering*, 1997.

[4] D.Langer. An integrated mmw radar system for outdoor navigation. In *Proceedings of the 1996 IEEE International conference on robotics and automation, Minneapolis, Minnesota*, April 1996.

[5] H. Durrant-Whyte. An autonomous guided vehicle for cargo handling applications. *Internation Journal of Robotics Research, Vol 15, No.5, October*, pages 407–440, 1996.

[6] P. Maybeck. *Stochastic Models, Estimation and Control*, volume 1. Academic Press, 1982.